

MARKOV CHAIN: A REALISTIC MODEL FOR TEMPORAL COENOSERE?

LÁSZLÓ ORLÓCI, MADHUR ANAND AND XIAOSHUANG HE
Department of Plant Sciences
The University of Western Ontario
LONDON, Canada N6A 5B7

SUMMARY

The lack of suitable analytical techniques to determine the transition matrix from survey-type data and to perform tests of significance that avoid reliance on theoretical distributions of dubious value, has hindered the application of the Markov chain model in descriptions of the serial change, called coenosere, in vegetation dynamics. This paper presents techniques and demonstrates their utility under realistic circumstances. Cases of functioning and fossil coenoseres are involved. The fact that the transition process in each is accurately described by a single transition matrix suggests the presence of significant Markovity of the stationary kind.

1. INTRODUCTION

We use the term "coenosere" to describe a set of vegetation states, and "temporal" to emphasize time as the ordering criterion. Our shorthand is $\mathbf{U}_1, \mathbf{U}_2, \dots, \mathbf{U}_c$ for the states in their chronological order and $\mathbf{X}_1, \mathbf{X}_2, \dots, \mathbf{X}_c$ for the c records that describe the states. The actual records can be ordinary phytosociological relevés (Braun-Blanquet 1932, Westhoff and van der Maarel 1973) for which we give examples in Tables 1,2,3. Table 1 contains annual descriptions of a heathland coenosere, Table 2 a coenosere without reference to exact chronological time, and Table 3 a fossil coenosere with sediment depth as a measure of time. We are interested in the description of these and other coenoseres in generalizable terms. We intend to show that the Markov chain is potentially useful for this purpose either as a postdictive or as a predictive

model, but only after the solution of two basic problems: measurement of transitions and Markovity testing.

Application of the Markov chain model entails many conceptual problems which Fekete (1985) describes under the circumstances of a vegetation study. In this paper, we focus on technical problems. We should mention that we use the approach of Waggoner and Stephens (1970) to visualize two-step and higher transitions, and randomization techniques that Edgington (1987) popularized to test hypotheses about Markovity.

2. FUNDAMENTAL NOTIONS

Our approach is contingent on the basic properties of a pure Markov coenosere and a conceptualization of population behaviour in the coenosere process:

2.1 THE MARKOV COENOSERE

2.1.1 When a coenosere is pure Markov, the description of its \mathbf{U}_{t+1} state can be derived from the relev  of its \mathbf{U}_t state and a known transition matrix \mathbf{P} :

$$\mathbf{X}_{t+1} = \mathbf{X}_t \mathbf{P} \quad \text{Eq. 1}$$

A typical element p_{hi} of the transition matrix expresses the rate at which population h loses ground to population i when the coenosere moves from one of its states to a future state. Based upon how far ahead the transitions are projected the transition matrix may be defined as one-step (\mathbf{P}), two-step (\mathbf{P}^2), three-step (\mathbf{P}^3), At one-step, transitions are examined over two adjacent states, at two-step over three states, at three-step over four states, The transition matrix may be constant or it may change in time. Based on this property, the coenosere (or Markov chain) is said to be "stationary" or "moving". A stationary coenosere keeps itself targeted on the same steady-state, while a moving coenosere undergoes retargeting from time to time by significant changes in the transition matrix. It is true that in the long run all coenoseres are "moving", but under the usual study scenario the time span is finite and coenosere stationarity is a valid question.

2.1.2 Any square matrix of non-negative numbers with unit row totals will qualify as a transition matrix \mathbf{P} and when \mathbf{X}_1 and \mathbf{P} are given, a stationary

Markov chain is completely defined (Feller (1968, Vol. I, p. 372 *et seq.*). It follows from the latter that it is sufficient to show that the coenosere is stationary, *i.e.*, it has a constant transition matrix, to show Markovity.,.

Conditions 2.1.1 and 2.1.2 give us a handle on method design, since they allow us to probe the coenosere for stationarity by way of simple comparisons of the observed coenosere to the Markov coenosere defined by the observed \mathbf{X}_1 and \mathbf{P} . We describe the steps in a later section.

2.2 POPULATION BEHAVIOUR AND TRANSITION MATRIX

Transitions can be derived from different types of data and by different techniques (*e.g.*, Waggoner and Stephens 1970, HORN 1975, USHER 1981, LIPPE, DE SMIDT AND GLEN-LEWIN 1985). The data may come from repeated surveys on the same site, or a one-time transect survey of different sites. Our technique assumes quantitative data which may be no more complicated than a set of phytosociological relevés on which transformations were performed to establish a homogeneous scale (WESTHOFF AND VAN DER MAAREL 1978). To present the technique, we focus on two states of the coenosere described by the relevés:

$$\mathbf{X}_j = \begin{bmatrix} X_{1j} \\ X_{2j} \\ \cdot \\ X_{ij} \\ \cdot \\ X_{rj} \end{bmatrix} \quad \mathbf{X}_k = \begin{bmatrix} X_{1k} \\ X_{2k} \\ \cdot \\ X_{ik} \\ \cdot \\ X_{rk} \end{bmatrix}$$

Considering the *i*th of *r* populations, it can have the following transitions from state \mathbf{U}_j to state \mathbf{U}_k :

- Type 1: $X_{ik} - X_{ij} > 0$: Population gains ground.
- Type 2: $X_{ik} - X_{ij} < 0$: Population loses ground.
- Type 3: $X_{ik} - X_{ij} = 0$: Population remains unchanged.

When a population gains ground, the resource it gains is no longer available to other competing populations. Our technique does in fact assume that all populations are competing for the same resource and any gain by population *i* is to the detriment of another population *h* even if

population h itself is gaining ground. In other words, population h does not have to be Type 2 to relinquish ground to population i.

The row (present) and column (future) entities of **P** are descriptions of the losses and gains of populations. When population i gains ground, label i in p_{hi} points to column i (see Fig. 1). When it loses ground, label i in p_{ih} points to row i. The value in the i,j cell, p_{ij} , is the amount of population i carried from state j to state k. The rate at which population h loses ground to population i, or equivalently, the rate at which population i gains ground from population h, is p_{hi} , the value in cell i of row h. The rate at which population i loses ground to population h is p_{ih} , the value in cell h of row i. We note that the sum of values in any one row of the transition matrix is set equal to 1 (or 100 %). This is consistent with the fact that through evolution of the coenosere every population carries its own biomass or it is replaced partially or completely by other populations.

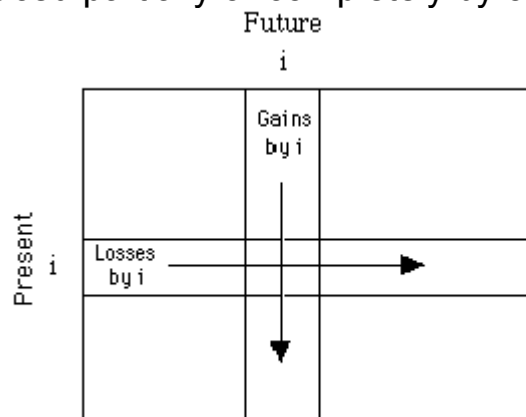


Figure 1. Interpretation of row i (present) and column i (future) in a transition matrix **P**. When population i is Type 1, it gains ground. The entries in column i indicate this gain on a population-to-population basis. When population i is Type 2, it suffers losses indicated in the i th row of **P**. All rows have unit sum. The column sums may be different.

Regarding the actual computations we assume that a changing population loses most to or gains most from the largest coexisting population. Accordingly, the basic equations for gain or loss by population i from or to population h is

$$DEV(i) = |X_{ik} - X_{ij}| \frac{X_{hk}}{X_{.k}} \quad \text{Eq. 2a}$$

when $h \neq i$ and

$$DEV(i) = X_{ik} \quad \text{Eq. 2b}$$

when $h = i$. In these X_{ik} , X_{hk} are quantities of population i and population h in relevé k and $X_{.k}$ is the sum of all values in relevé k. Eq. 2 may seem an over-simplification of the process, but this is as much as we can realistically say about transitions from ordinary relevés.

2.3 THE ARITHMETIC OF TRANSITIONS

To show the arithmetic of transition computations¹, we give step-by-step results for the data set

46.7222	27.3256	16.6667	0
33.4027	36.3372	25	50
19.8751	36.3372	58.3333	50

This is the **X** matrix of four relevés (columns as time steps) described by 3 species (rows). The elements are percentages. The following illustrates the computations (automatic in program FitMarko) that yield the one-step² transition matrix **P**₁ for relevé 1 to 2:

1. At $i=1$, $DEV1 = 27.3256 - 46.7222 = -19.3966$. Since $DEV1$ is negative, $i=1$ points to row 1 in **P**₁. The initial elements in row 1 are

$$\begin{aligned}p_{111} &= 27.3256 \\p_{112} &= 19.3966 \times 36.3372/100 = 7.04818 \\p_{113} &= 19.3966 \times 36.3372/100 = 7.04818\end{aligned}$$

2. At $i=2$, $DEV2 = 36.3372 - 33.4027 = 2.9345$. $DEV2$ is positive and $i=2$ points to column 2 in **P**₁. The elements of column 2 are modified:

$$\begin{aligned}p_{112} &= 7.04818 + 2.9345 \times 27.3256/100 = 7.85005 \\p_{122} &= 36.3372 \\p_{132} &= 2.9345 \times 36.3372/100 = 1.06632\end{aligned}$$

3. At $i=3$, $DEV3 = 36.3372 - 19.8751 = 16.462$. $DEV3$ is positive and $i=3$ points to column 3 in **P**₁. The elements in column 3 become

$$\begin{aligned}p_{113} &= 7.04818 + 16.4621 \times 27.3256/100 = 11.5465 \\p_{123} &= 16.4621 \times 36.3372/100 = 5.98186 \\p_{133} &= 36.3372\end{aligned}$$

¹We are presenting the results of longhand calculations and these should be suitable to verify the automatic computations performed by program FitMarko. In the interest of compatibility, we are required to work with what appears to be an over-excess of digits. This should not imply a level of accuracy in the numbers beyond the accuracy in the raw observations.

²The computational task is the same at any step size. FitMarko makes provision for this by requesting specification of an upper limit for step size. At step size 1 the transitions (j to k in Eq. 3a) go from state **U**₁ to **U**₂, **U**₂ to **U**₃, ... , at step size 2 from **U**₁ to **U**₃, **U**₂ to **U**₄, ... and on in the same manner.

4. Based on the preceding steps, the initial \mathbf{P}_1 matrix is

27.3256	7.85005	11.5465
0	36.3372	5.98186
0	1.06632	36.3372

After normalization of rows, \mathbf{P}_1 becomes

0.58485	0.16802	0.24713
0.00000	0.85865	0.14135
0.00000	0.02851	0.97149

5. Similar computations yield the \mathbf{P}_2 and \mathbf{P}_3 transition matrices:

0.57048	0.09121	0.33831
.04845	0.64099	0.31056
0.00000	0.00000	1.00000

and

0.00000	0.50000	0.50000
0.00000	1.00000	0.00000
0.00000	0.25000	0.75000

6. The average of \mathbf{P}_1 , \mathbf{P}_2 , \mathbf{P}_3 is the \mathbf{P} matrix sought:

0.47506	0.20353	0.32141
0.01439	0.84782	0.13779
0.00000	0.10919	0.89081

2.4. FITTING THE MODEL

Program FitMarko takes \mathbf{P} and relevé \mathbf{X}_1 (first column vector of \mathbf{X}) and generates Markov relevés $\mathbf{M}_2, \dots, \mathbf{M}_c$ according to

$$\mathbf{M}_k = \mathbf{M}_j \mathbf{P} \quad \text{Eq. 3}$$

Note that $\mathbf{M}_1 = \mathbf{X}_1$. FitMarko then takes $\mathbf{X}_1, \mathbf{X}_2, \dots, \mathbf{X}_c$ and $\mathbf{M}_1, \mathbf{M}_2, \dots, \mathbf{M}_c$, computes two $c \times c$ distance matrices \mathbf{D}_X and \mathbf{D}_M and determines the level of stress (discordance) between \mathbf{D}_X and \mathbf{D}_M as the square root of

$$\sigma^2(\mathbf{D}_X; \mathbf{D}_M) = \frac{\sum_{j < k}^c (d_{Xjk} - d_{Mjk})^2}{\sum_{j < k}^c (d_{Xjk} + d_{Mjk})^2} \quad \text{Eq. 4}$$

This is proportional to the closeness of the Markov model and the observed coenosere in distance configuration terms. Symbol d represents a structure neutral Euclidean distance³. The \mathbf{D}_X and \mathbf{D}_M matrices and the $\sigma(\mathbf{D}_X; \mathbf{D}_M)$ values are the basis of further computations which probe the observed coenosere for stationarity and Markovity.

2.5 TESTS ON THE OBSERVED COENOSERE

As a complication, stress values are interpretable only in terms of a scale on which we can measure their relative size. It is convenient to make this a probability scale associated with the sampling distribution of stress (Eq. 4) under a null hypothesis (H_0). The latter will depend on the properties whose existence we try to detect. Program FitMarko provides two options for H_0 :

2.5.1 H_0 : COENOSERE UNDIRECTED

A coenosere of this sort is chaotic (that is zero order Markov) in that each state transits to another by way of a different transition matrix. This state of chaos represents an extreme case which we can simulate by random permutations of the observed relevés. Each permutation (possible total number of $c!$) gives rise to a new stress value. After many permutations of original or permuted \mathbf{X} , the generated stress values collectively form a sampling distribution. It is a fact that stress increases as the transitions become more and more chaotic. Accordingly, we reject H_0 if the proportion of simulated stress values equal to or smaller than the observed $\sigma(\mathbf{D}_X; \mathbf{D}_M)$ is smaller than a threshold, say 0.1, 0.05, or 0.01. After rejection of H_0 , stationarity is assumed, and according to criterion 2.1.2 Markovity is accepted at the step size for which the transition matrix is defined.

³A distance function is called structure neutral if it does not involve data transformations that affect structural changes in the reference space of the analysis.

2.5.2 H_0 : COENOSERE MARKOV WITH m -STEP TRANSITION MATRIX

A formal test under this option may rely on the known fact that in a pure Markov coenosere the expectation of a $2m$ -step transition matrix \mathbf{P}^{2m} is the product of the m -step transition matrix \mathbf{P}^m with itself, that is, H_0 : $E(\mathbf{P}^{2m}) = \mathbf{P}^m \mathbf{P}^m$. If H_0 is found tenable, the Markov chain is shown to be of order m . We contemplated a direct simulation approach for the test, but the problem of the outcome depending on the scaling factor that we had to apply to the transition values in order to create a base for random sampling forced us to choose another approach. In this, we obtain Markov relevés \mathbf{M} (grand total $f..$) according to Eq. 3 based on an m -step transition matrix and then we stretch \mathbf{M} by way of an array \mathbf{u} of $f..$ cells in such a way that the code of an element of \mathbf{M} will appear in a specific number of cells equal to the value of the element. We sample array \mathbf{u} at random $f..$ times and summarize the outcome in a new \mathbf{M} matrix. We repeat the sampling a specific large number of times and we compute a new stress value for each sample. Noting that stress increases as the arrangement becomes more and more unlike the Markov of order m , we reject H_0 if the proportion of the simulated stress values at least as large as the observed $\sigma(\mathbf{D}_X; \mathbf{D}_M)$ is smaller than a specified threshold, say 0.10, 0.05, 0.01. Rejection leads to the conclusion that the coenosere is not Markov of order m .

2.5.3 COMPARISON OF TEST OPTIONS

Option 5.2 uses a very restrictive null hypothesis. The alternative hypothesis, Markovity under 5.1, is more likely to be accepted than the null hypothesis, Markovity of a specified order under option 5.2. The possible lack of a simple agreement between the two tests poses a dilemma, namely, how to interpret the outcomes if Markovity is concluded under option 5.1 and rejected at the same step size under option 5.2. We can suggest that the results are still valid in the sense that while option 5.1 takes even weak manifestations of Markovity as indications of Markovity, option 5.2 rejects Markovity unless its manifestations are strong. It will therefore be our practice to characterize a coenosere as being weakly Markov if rejection of the null hypothesis under 5.1 is not corroborated by acceptance of the null hypothesis under 5.2.

3. RESULTS

3.1 HEATHLAND RECOVERY

3.1.1 TRANSITION MATRICES

We performed one-step, two-step and three-step analyses on the data set in Table 1 by program FitMarko and obtained 18 one-step, 17 two-step and 16 three-step transition matrices. The average of the 18 one-step transition matrices⁴ is:

```
.76480 .13945 .05628 .02656 .00116 .00455 .00148 .00339 .00234  
.01323 .95375 .01660 .00688 .00154 .00344 .00143 .00045 .00268  
.01304 .05180 .92028 .00606 .00134 .00325 .00130 .00044 .00250  
.01924 .11058 .04133 .81922 .00128 .00413 .00146 .00060 .00217  
.02685 .12406 .04602 .01709 .77525 .00476 .00188 .00063 .00345  
.03093 .13603 .05083 .01703 .00158 .75754 .00172 .00149 .00284  
.04221 .15201 .06296 .01743 .00191 .00460 .71411 .00139 .00338  
.09055 .17091 .07742 .04942 .00067 .00549 .00139 .60338 .00077  
.02908 .18118 .06217 .01409 .00186 .00509 .00235 .00054 .70364
```

This is matrix **P**. A typical element 0.11058, 4th row 2nd cell, is the rate at which, on average, *Erica tetralix* loses ground to *Empetrum nigrum* during annual transitions. The element in the same position of **P**² or **P**³ below indicates the rates at which *Erica tetralix* loses ground to *Empetrum nigrum* under biannual and triannual transitions. The average of the 17 two-step transition matrices is:

```
.63289 .22337 .08679 .04207 .00164 .00462 .00178 .00351 .00333  
.01673 .94687 .02044 .00674 .00186 .00258 .00143 .00042 .00293  
.01620 .07294 .89534 .00672 .00167 .00241 .00138 .00040 .00294  
.02570 .17993 .06508 .71836 .00187 .00370 .00178 .00046 .00311  
.02945 .14059 .05014 .01409 .75626 .00344 .00202 .00058 .00343  
.02579 .12123 .04296 .01420 .00216 .78892 .00174 .00043 .00257  
.03318 .18660 .06855 .01396 .00220 .00419 .68668 .00050 .00414  
.13042 .29047 .12969 .07630 .00100 .00572 .00183 .36221 .00236  
.03196 .20679 .06767 .01175 .00235 .00384 .00149 .00051 .67364
```

This is **P**². The average of the three-step transition matrices is:

```
.55121 .27507 .11313 .04469 .00226 .00614 .00259 .00114 .00377
```

⁴In this case and in all the others which involve copies of a computer written file, we give the numbers without rounding or truncation.

.01545 .94336 .02645 .00416 .00184 .00327 .00166 .00039 .00342
.01594 .09791 .87160 .00451 .00169 .00321 .00156 .00037 .00322
.02708 .22433 .08404 .65075 .00217 .00510 .00232 .00034 .00386
.03007 .15436 .05271 .00942 .74301 .00473 .00195 .00047 .00330
.02396 .15025 .04706 .00816 .00188 .76323 .00180 .00045 .00322
.03421 .21790 .07497 .00991 .00204 .00573 .65052 .00035 .00437
.15956 .40587 .18268 .09850 .00265 .00710 .00310 .13638 .00415
.03191 .19852 .06691 .01174 .00235 .00459 .00193 .00062 .68143

This is the \mathbf{P}^3 . The numbers above are copied directly from a computer file. Note that the number of rows and columns is equal to the number of descriptors (bare ground and plant populations) of the coenosere. This is the same for any step size. Note also that the transition matrices have unit row sums (within rounding errors).

Table 1. Percentage point cover for bare ground and plant populations in 19 annual records of heathland vegetation undergoing recovery from the effects of severe fire (after LIPPE, DE SMIDT AND GLEN-LEWIN 1985, their Table 1). Species code: BG - bare ground, EN - *Empetrum nigrum*, CV - *Caluna vulgaris*, ET - *Erica tetralix*, MC - *Molinia caerulea*, CP - *Carex pilulifera*, JS - *Juncus squarrosus*, RA - *Rumex acetosella*, OS - other species. With moderate reversals in 1977 and 1978, bare ground and most species exhibit monotonic gains or losses through the recording period.

Year	BG	EN	CV	ET	MC	CP	JS	RA	OS
1963	57.1	17.9	8.6	11.6	0.0	0.2	0.0	4.7	0.0
1964	44.0	25.0	13.7	12.2	0.0	1.1	0.2	3.9	0.0
1965	32.7	34.9	13.9	14.3	0.0	0.5	0.0	3.7	0.0
1966	27.5	36.8	20.0	14.1	0.1	0.9	0.2	0.3	0.1
1967	19.7	46.1	21.0	10.8	0.1	0.7	0.4	0.5	0.7
1968	10.7	54.2	22.2	10.6	0.7	0.6	0.4	0.0	0.5
1969	6.7	55.7	23.3	10.4	0.3	2.0	0.7	0.1	0.7
1970	5.8	61.1	23.7	6.9	0.2	1.2	0.7	0.2	0.3
1971	9.5	57.6	24.7	6.6	0.4	0.6	0.4	0.0	0.3
1972	8.4	62.1	23.7	3.6	0.3	1.2	0.1	0.0	0.6
1973	4.4	67.9	21.3	3.3	0.2	0.6	0.4	0.0	2.0
1974	8.5	58.1	25.8	4.7	0.6	1.3	0.7	0.0	0.4
1975	9.2	62.2	24.3	2.5	0.6	0.9	0.2	0.0	0.1
1976	9.9	58.2	24.9	3.7	0.6	1.1	0.7	0.0	1.0
1977	19.6	48.4	23.5	5.7	0.3	1.2	0.4	0.1	0.9
1978	12.1	58.1	22.7	4.8	0.4	0.4	0.0	0.2	1.3
1979	9.3	65.1	20.3	2.7	0.0	1.5	0.1	0.2	0.9
1980	7.3	68.2	21.5	1.2	0.5	1.0	0.1	0.1	0.2
1981	5.4	65.5	20.8	4.6	1.0	1.6	0.4	0.3	0.6

3.1.2 MARKOV RELEVÉS

Repeated application of Eq. 1 generates the Markov relevés. Note that \mathbf{M}_1 is \mathbf{X}_1 (relevé 1 below). Premultiplication of \mathbf{P} by \mathbf{X}_1 gives rise to Markov relevé \mathbf{M}_2 , Premultiplication of \mathbf{P} by \mathbf{M}_2 produces \mathbf{M}_3 , and so on.

The computations continue until a certain level of stability is reached at which point the iterations stop. Only selected Markov relevés are given:

Relevé: **M1=X1**

57.043 17.8821 8.59141 11.5884 0 .1998 0 4.6953 0

Relevé: **M2**

44.6295 27.5658 12.2663 11.4189 .123625 .573875 .144623 3.04537 .231991

Instability level at this step= 16.259 or 100 %

Instability reduction= 0 %

Relevé: **M3**

35.1867 35.0905 15.0238 10.972 .224842 .838751 .247037 2.01461 .401763

Instability level at this step= 12.4408 or 76.5164 %

Instability reduction= 23.4836

Relevé: **M4**

28.0185 40.9626 17.0918 10.3831 .307281 1.02564 .319504 1.3657 .525948

Instability level at this step= 9.53786 or 58.6622 %

Instability reduction= 17.8542

(Intermediate steps not given)

Relevé: **M12**

8.10456 59.6424 22.4854 6.20627 .590125 1.42748 .482767 .222111 .838888

Instability level at this step= 1.26578 or 7.78515 %

Instability reduction= 2.10041%

(Intermediate steps not given)

Relevé: **M19**

6.06077 62.7648 22.6886 4.88407 .635663 1.43791 .492219 .169237 .866734

Instability level at this step= .277578 or 1.70723 %

Instability reduction= .374665 %

(Intermediate steps not given)

Relevé: **M22**

5.86757 63.2561 22.6091 4.66193 .641504 1.43644 .492784 .165128 .869476

Instability level at this step= .159257 or .979502 %

Instability reduction= .191491%

Instability level reduced below 1%. Iterations stopped.

Note the instability levels given after each iteration. These indicate the magnitude of discordance between a current Markov relevé and the stable Markov relevé on which the Markov coenosere converges⁵. Stability is closely approached in 19 steps. The similarity of the deemed stable state (**M₂₂** above) and the 1981 relevé in Table 1 is remarkable. The computations differ somewhat in the two-step and three-step case. In the two-step case $\mathbf{M}_1 = \mathbf{X}_1$, $\mathbf{M}_2 = \mathbf{X}_1 \mathbf{P}$, $\mathbf{M}_3 = \mathbf{X}_1 \mathbf{P}^2$, $\mathbf{M}_4 = \mathbf{M}_2 \mathbf{P}^2$, and in the

⁵The computations stop at minimum instability if convergence cannot bring the instability level down to the specified value given in the startup dialogue of FitMarko.

three-step case $\mathbf{M}_1 = \mathbf{X}_1$, $\mathbf{M}_2 = \mathbf{X}_1 \mathbf{P}$, $\mathbf{M}_3 = \mathbf{X}_1 \mathbf{P}^2$, $\mathbf{M}_4 = \mathbf{X}_1 \mathbf{P}^3$, $\mathbf{M}_5 = \mathbf{M}_2 \mathbf{P}^3$,
...

3.2 TESTS ON MARKOVITY

We now give a summary of the complete analysis:

3.2.1 One-step case, testing option 5.1. The stress level $\sigma(\mathbf{D}_X; \mathbf{D}_M)$ is 0.24. This value could be given as 24% if we followed the practice of engineers, but we forgo such a practice simply because the stress scale is an open-ended percentage scale on which values greater than 100% may occur. We take probabilities from the sampling distribution of stress as our standard scale. In these terms, the proportions of stress values expected to be equal to or less than 0.24 under the null hypothesis of an chaotic coenosere is less than 0.01. Accordingly, we reject the null hypothesis and declare the heathland coenosere directed in a Markovian fashion. The mean of the generated stress values is 1.07 and its standard deviation is 0.011. Expressed as a deviation from the mean in standard units, the observed stress is $Z=-75.45$.

3.2.2 One-step case, testing option 5.2. The stress level is the same as above. The proportions of generated stress values at least as large as 0.24 under the null hypothesis of first order Markovity is 0.99. Consistent with testing option 5.2, we modify our conclusion of testing option 5.1 and declare the heathland coenosere strongly Markovian of first order. The mean of the generated stress values is 0.33 and its standard deviation is 0.0047. Expressed as a deviation from the mean in standard units, the observed stress is $Z=-19.15$.

3.2.3 Other cases. Continuing in the same manner, we reject the null hypothesis of a chaotic two-step or three-step coenosere at critical probability levels 0.01 and less than 0.01 (testing option 5.1). In the test of second and third order Markovity (testing option 5.2) the critical probabilities are respectively 0.85 and 0.67, both missing significance by being too large. Thus we accept the null hypothesis of strong Markovity at these orders.

3.3 SIGNATURES OF MARKOVITY AND CHAOS

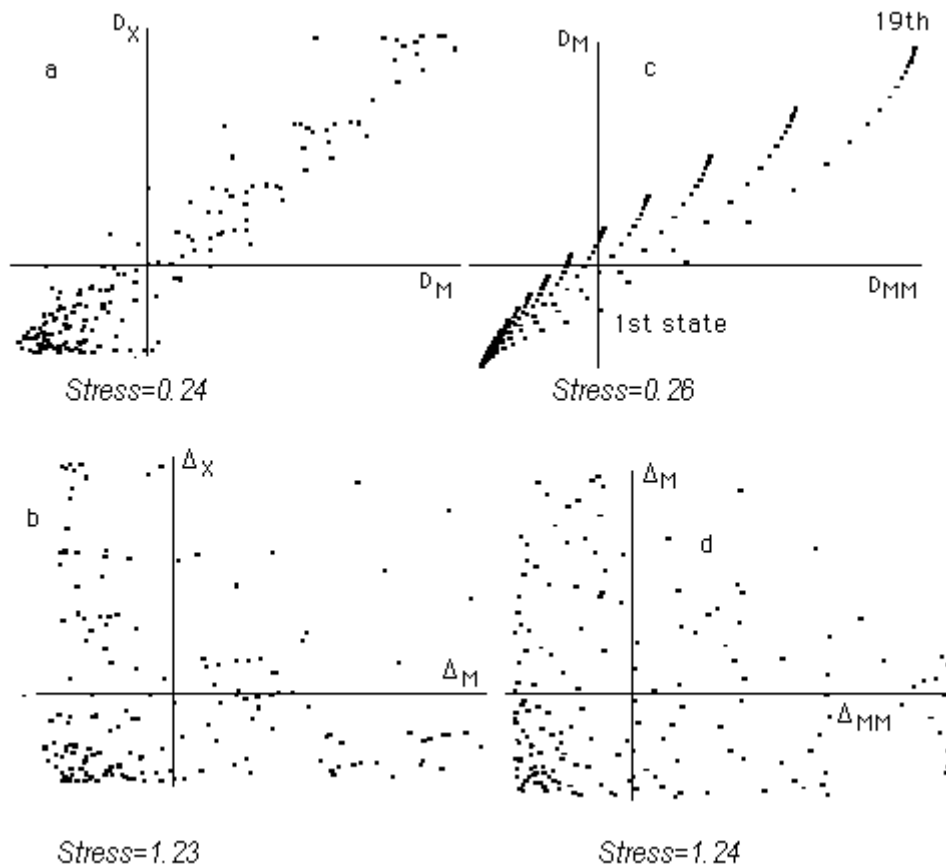
Our conclusions about Markovity are reinforced by specific structural characteristics in the sample revealed by the joint plot of distance values in Fig. 2. Distance values from the one-step \mathbf{D}_X and \mathbf{D}_M matrices are the coordinates in graph *a*. Graph *b* uses distances from Δ_X and Δ_M which we compute from a random permutation of the columns in \mathbf{X} as coordinates. The \mathbf{D}_X and \mathbf{D}_M configurations are strongly concordant as seen in graph *a* and their stress value is low. Discordance is complete in graph *b* and the stress value (Eq. 4) is high. These reconfirm our earlier observation that an increased lack of directedness in the transitions generate increased values of stress.

Graph *c* displays the joint scatter of the Markov distances (\mathbf{D}_M) and corresponding Markov-Markov (\mathbf{D}_{MM}) distances. We generate \mathbf{D}_{MM} by reanalysis of the Markov relevés. Graph *d* displays the joint scatter of the Δ_M and Δ_{MM} distances. Note the increased crowding of points in graph *c* along the runs upwards and from right to left. This is the signature of a pure Markov coenosere. Graph *c* reveals a signature of chaos.

The first run of points in graph *c* begins with a point near the vertical axis just left and up from "1st state". One coordinate of this point is the distance of the first Markov relevé and the second Markov relevé (the first nonzero element in \mathbf{D}_M). The other coordinate of the same point is the distance of the first Markov-Markov relevé and the second Markov-Markov relevé (the first nonzero element in \mathbf{D}_{MM}). The last point in the run, the topmost on the right, has the distance of the first Markov relevé and the 19th Markov relevé as one of its coordinates and the distance of the first Markov-Markov relevé and the 19th Markov-Markov relevé as its second coordinate. The points in the second run in graph *c* have the distances of the 2nd Markov relevé and 2nd Markov-Markov relevé with the 3rd, 4rd, etc. as coordinates. This pattern is repeated throughout the graph. The point on the extreme left has the distance of the 18th and 19th Markov relevés and the 18th and 19th Markov-Markov relevés as coordinates.

The stress values of configurations *a* and *c* are practically identical. Interestingly, graph *a* can be derived by about 12% random distortion of graph *c*. Graphs *b* and *d* are identical in being random configurations. We regard graphs *a* as a signatures of Markovity somewhat distorted by random variation superimposed on the point configuration. The idea that configuration *a* is derivable from configuration *c* by superimposing random variation on *c* is consistent with the results of canonical contingency table

Figure 2. Joint scatter of relevé distances based on analysis of the data in Table 1 (graphs *a* and *b*) and reanalysis of the Markov relevés (graphs *c* and *d*). The horizontal axis depicts the D_M configuration in *a* and *b* and the D_{MM} configuration in *c* and *d*. The vertical axis depicts the D_X configuration in *a* and *b* and the D_M configuration in *c* and *d*. Each graph contains 171 points. Graph *b* and *d* show the effects of randomization. Graph *c* is the signature of the pure Markov process. Graph *a* is the signature of the observed configuration. The latter is similar to the Markov signature with about 12% random variation superimposed. The definition of stress correspond to Eq. 4 in the text.



analysis (Orlóci, 1991) which we performed on each configuration. The percentages of the total variation accounted for by the largest eigenvalue (squared canonical correlation) in each configuration are as follows:

Configuration (Fig. 1)	<i>a</i>	<i>b</i>	<i>c</i>	<i>d</i>
% of total variation accounted for	88	11	100	11

It is seen that the pure Markov configuration M corresponding to graph *c* has a single eigenvalue. The observed configuration X corresponding to graph *a* has several eigenvalues, but only one is dominant. This dominant Eigenvalue accounts for only 12% less of the total variation than the single Eigenvalue in the pure Markov configuration. The random configurations

(b, d) have several small Eigenvalues more or less equal. Clearly in these terms, the heathland coenosere carries the unmistakable signature of a stationary Markov chain.

3.4 FROM PASTURE LAND TO CLIMAX FOREST

Cooper (1922, also Braun-Blanquet 1932, p.333) described the dynamics of six shrub species that he considered characteristic in secondary succession on pasture land in a New England site. Cooper's data are recapitulated in Table 2. The averaged one-step transition values are

.36180	.11131	.15285	.16379	.12381	.08645
.03023	.53852	.09682	.12621	.12621	.08200
.00000	.01274	.61740	.10093	.16750	.10142
.00000	.00000	.02282	.79823	.11109	.06787
.00000	.00000	.01230	.02224	.87011	.09534
.00000	.00000	.01332	.02738	.14263	.81667

Table 2. Frequency changes in six shrub species during secondary succession in a New England plant community. Frequencies were transcribed from Cooper's block diagram in Braun-Blanquet (1932, Fig. 169). Row totals are adjusted. Species symbols: ST - *Spiraea tomentosa*, JC - *Juniperus communis*, CR - *Corylus rostrata*, HV - *Hamamelis virginiana*, VA - *Viburnum alnifolia*, TC - *Taxus canadensis*.

Successional stage	Species					
	ST	JC	CR	HV	VA	TC
Scrub stage	44.9	32.1	19.1	1.3	1.3	1.3
Pinus strobus forest	18.8	25.0	25.0	18.8	6.2	6.2
Mixed forest	8.0	12.0	28.0	20.0	20.0	12.0
Climax forest	0.0	5.3	5.3	21.0	42.1	26.3

Using the first column in Table 2 as the startup relevé, Markov relevé \mathbf{M}_6 is

0.63709 3.10694 9.22519 20.8581 40.2906 25.8821

This delineates a composition similar to the composition of the shrub layer in Cooper's climax community. It should be noted that \mathbf{M}_6 is still far from the stable state which is closely approached by \mathbf{M}_{17} ,

0.00605156 0.110788 3.62966 12.8344 50.7216 32.6975

The stable Markov relevé has less of *Juniperus* and *Corylus*, much less of *Hamamelis*, and more of *Viburnum* and *Taxus* than the quantities given for the climax community. How reliable is the Markov model in this example? The observed stress value is 0.34 ($Z = -8.05$). The probability of a stress value as small or smaller than 0.34 occurring under the null hypothesis of chaotic transitions is about 0.08. The stress and critical probability in the two-step case are 0.35 and 0.04. Although the probability in the one-step case is not small, in the two-step case it is well within the limits to indicate rejection of the null hypothesis and acceptance of the alternative that the coenosere is Markov in line with testing option 5.1.

The observed stress values for first and second order Markovity are the same as the stress values above. The critical probabilities are zero. Consistent with testing option 5.2 we reject the notion of Markovity of the specified orders and declare weak Markovity on the observed coenosere in the light of the outcome under testing option 5.1. The small number of time steps is noted which makes the conditions suboptimal for testing.

3.5 THE POSTGLACIAL TIME SCALE

Delcourt and Delcourt (1985) present fossil-pollen diagrams for Anderson Pond in Tennessee. The diagrams trace compositional changes in the region's vegetation over a time span of 20,000 years. We give the reconstructed data in Table 3 for which the average one-step transition matrix is

.63509	.07117	.01972	.05542	.01458	.15073	.05329
.07318	.65585	.02172	.05165	.00998	.12990	.05773
.64686	.04633	.02140	.06296	.01418	.14819	.06007
.06195	.62499	.03290	.06036	.01176	.13953	.06850
.00217	.02635	.86982	.02070	.01177	.05163	.01755
.00320	.01666	.03775	.80778	.01838	.09471	.02151
.00231	.01594	.04605	.01646	.86103	.04479	.01341
.00088	.01611	.04299	.02726	.01573	.87971	.01732
.01313	.01305	.01932	.06014	.02365	.20302	.66769

FitMarko postdicts the stable state (\mathbf{M}_{19}) to contain fossil-pollen of the 9 taxa approximately in the proportions of

1.5258 4.78321 22.1873 13.4385 9.59913 42.5027 5.96331

These reproduce roughly the observed profile under "present" in Table 3. The one-step stress level is 0.44 ($Z = -57.06$). The probability of a stress value as small or smaller than 0.44 under the null hypothesis of chaotic transitions is less than 1%. We concluded that the coenosere is Markovian (testing option 5.1). In the two-step and three-step case the stress values are respectively 0.38 and 0.37. These indicate rejection of the hypothesis of chaotic two- or three-step transitions. The tests on one- to three-step Markovity lead to rejection of the null hypothesis with the conclusion that the fossil coenosere is weakly Markovian (testing option 5.2).

Table 3. Arboreal pollen counts in lake sediment transcribed from Fig. 3.2 in Delcourt and Delcourt (1987). The locality is Anderson Pond, Tennessee. The time span is 20,000 years.

Taxon	20,000 B.P.								Present	
Picea	30	40	20	10	10	5	5	1	1	0
Pinus	75	75	35	10	5	5	2	5	5	10
Acer	0	1	5	5	5	5	5	5	5	30
Fraxinus	1	5	15	10	15	20	30	25	20	10
Carya	1	1	1	5	5	5	10	10	10	10
Quercus	5	5	30	40	65	50	70	70	70	40
Ostrya *	1	1	15	25	20	5	5	5	1	1

* Also, Carpinus

4. DISCUSSION

We have set as one objective the design of a technique by which we can determine transition matrices from vegetation data given in the form of ordinary Braun-Blanquet relevés. Being able to handle relevés of this kind has considerable utility. To see this point, it is sufficient to observe that vegetation surveys have routinely used and still are using relevés of this type, and that vast amounts of records in data banks also have this relevé format.

We referred to a chronologically ordered set of relevés as a temporal coenosere. We gave examples to illustrate the diversity of sources from which such a coenosere may emerge, used observed transition matrices to fit the Markov chain, and applied randomization tests to probe the data for Markovity. The test procedure involved 3 steps: first, measurement of discordance between an observed coenosere and the fitted Markov coenosere in terms of a stress function defined for distance matrices; second, experimental derivation of a probability distribution for stress

under the null hypothesis of chaotic transitions, and three, similar derivation of a sampling distribution of stress under the null hypothesis of Markovity of specified order. The stress function signaled maximum discordance when the transitions were chaotic. Accordingly, our decision rule required rejection of the chaotic transitions hypothesis when the probability of obtaining a stress value equal to or less than the observed stress value under the assumption of chaotic transitions was small. Rejection led to acceptance of the alternative that the coenosere was in fact Markov justified by the fact that it is describable by a stationary transition matrix (criterion 2.1.2). Rejection of the null hypothesis of an m-order Markov coenosere required that the probability of a stress value as large or larger than the observed stress value under the null hypothesis be small. Rejection of the chaotic transitions hypothesis followed by rejection of the mth order Markovity hypothesis lead to acceptance of weak Markovity in the coenosere. Acceptance of the mth order Markovity hypothesis lead to acceptance of strong Markovity in the coenosere. Based on the tests we succeeded to show strong Markovity in the heathland coenosere and weak Markovity in the other data.

For availability of program FitMarko interested readers should contact the office of the first author.

REFERENCES

BRAUN-BLANQUET, J. 1932. **Plant Sociology**. Translated and published by G. D. Fuller and H. S. Conard, New York.

COOPER, W.S. 1922. The ecological life history of certain species of *Ribes*. *Ecology* 3:7-16.

DELCOURT P.A., DELCOURT H.R. 1985. **Long-term forest dynamics of the temperate zone**. Springer-Verlag, New York.

EDGINGTON, E.S. 1987. **Randomization Testing**. Marcel Dekker, New York.

FELLER, W. 1968. **An Introduction to Probability Theory and Its Applications**. 3rd ed. Wiley, New York.

FEKETE, G. 1985. Terrestrial vegetation succession: theories, models, reality. In **Problems of Coenological Succession** (In Magyar. G. Fekete ed.) Akadémiai Kiadó, Budapest, pp. 31-63.

HORN, H.S. 1975. Markovian properties of forest succession. In **Ecology and evolution of communities** (M.L. Cody and M.J. Diamond eds.) Harvard University Press, Cambridge, Massachusetts, pp. 196-211.

LIPPE E., DE SMIDTS, J.T. GLEN-LEWIN D.C. 1985. Markov models and succession: a test from a heathland in the Netherlands. **Journal of Ecology** 73, 775-791.

ORLÓCI L. 1991. **Conapack: program for canonical analysis of classification tables**. Ecological Computations Series (CS), Vol. 4, SPA Academic Publishing, The Hague, The Netherlands.

ORLÓCI L. Orlóci M. 1988. On recovery, Markov chains, and canonical analysis. **ECOLOGY** 69, 1260-1265.

RÉNYI, A. 1961. On measures of entropy and information. In **Proceedings of the 4th Berkeley Symposium on mathematical statistics and probability** (J. Neyman ed.) University of California Press, Berkeley, pp. 547-561.

USHER, M.B. 1981. Modelling ecological succession, with particular reference to Markovian model. *Vegetatio* 46:11-18.

WAGGONER, P. E., G. R. STEPHENS. 1970. Transition probabilities for a forest. *Nature* 225: 1160-1161.

WESTHOFF V., E. VAN DEER MAAREL. 1973. The Braun-Blanquet approach. In **Classification of plant communities** (R. H. Whiter ed.) Dr. W. Junk, The Hague, The Netherlands, pp. 287-399.

Table 1. Percentage point cover for bare ground and plant populations in 19 annual records of heathland vegetation undergoing recovery from the effects of severe fire (after LIPPE, DE SMIDT AND GLEN-LEWIN 1985, their Table 1). Species code: BG - bare ground, EN - *Empetrum nigrum*, CV - *Caluna vulgaris*, ET - *Erica tetralix*, MC - *Molinia caerulea*, CP - *Carex pilulifera*, JS - *Juncus squarosus*, RA - *Rumex acetosella*, OS - other species. With moderate reversals in 1977 and 1978, bare ground and most species exhibit monotonic gains or losses through the recording period.

Year	BG	EN	CV	ET	MC	CP	JS	RA	OS
1963	57.1	17.9	8.6	11.6	0.0	0.2	0.0	4.7	0.0
1964	44.0	25.0	13.7	12.2	0.0	1.1	0.2	3.9	0.0
1965	32.7	34.9	13.9	14.3	0.0	0.5	0.0	3.7	0.0
1966	27.5	36.8	20.0	14.1	0.1	0.9	0.2	0.3	0.1
1967	19.7	46.1	21.0	10.8	0.1	0.7	0.4	0.5	0.7
1968	10.7	54.2	22.2	10.6	0.7	0.6	0.4	0.0	0.5
1969	6.7	55.7	23.3	10.4	0.3	2.0	0.7	0.1	0.7
1970	5.8	61.1	23.7	6.9	0.2	1.2	0.7	0.2	0.3
1971	9.5	57.6	24.7	6.6	0.4	0.6	0.4	0.0	0.3
1972	8.4	62.1	23.7	3.6	0.3	1.2	0.1	0.0	0.6
1973	4.4	67.9	21.3	3.3	0.2	0.6	0.4	0.0	2.0
1974	8.5	58.1	25.8	4.7	0.6	1.3	0.7	0.0	0.4
1975	9.2	62.2	24.3	2.5	0.6	0.9	0.2	0.0	0.1
1976	9.9	58.2	24.9	3.7	0.6	1.1	0.7	0.0	1.0
1977	19.6	48.4	23.5	5.7	0.3	1.2	0.4	0.1	0.9
1978	12.1	58.1	22.7	4.8	0.4	0.4	0.0	0.2	1.3
1979	9.3	65.1	20.3	2.7	0.0	1.5	0.1	0.2	0.9
1980	7.3	68.2	21.5	1.2	0.5	1.0	0.1	0.1	0.2
1981	5.4	65.5	20.8	4.6	1.0	1.6	0.4	0.3	0.6

Table 2. Frequency changes in six shrub species during secondary succession in a New England plant community. Frequencies were transcribed from Cooper's block diagram in Braun-Blanquet (1932, Fig. 169). Row totals are adjusted. Species symbols: ST - *Spiraea tomentosa*, JC - *Juniperus communis*, CR - *Corylus rostrata*, HV - *Hamamelis virginiana*, VA - *Viburnum alnifolia*, TC - *Taxus canadensis*.

Successional stage	Species					
	ST	JC	CR	HV	VA	TC
Scrub stage	44.9	32.1	19.1	1.3	1.3	1.3
Pinus strobus forest	18.8	25.0	25.0	18.8	6.2	6.2
Mixed forest	8.0	12.0	28.0	20.0	20.0	12.0
Climax forest	0.0	5.3	5.3	21.0	42.1	26.3

Table 3. Arboreal pollen counts in lake sediment transcribed from Fig. 3.2 in Delcourt and Delcourt (1987). The locality is Anderson Pond, Tennessee. The time span is 20,000 years.

Taxon	20,000 B.P.									Present
	30	40	20	10	10	5	5	1	1	
Picea	30	40	20	10	10	5	5	1	1	0
Pinus	75	75	35	10	5	5	2	5	5	10
Acer	0	1	5	5	5	5	5	5	5	30
Fraxinus	1	5	15	10	15	20	30	25	20	10
Carya	1	1	1	5	5	5	10	10	10	10
Quercus	5	5	30	40	65	50	70	70	70	40
Ostrya *	1	1	15	25	20	5	5	5	1	1

* Also, Carpinus

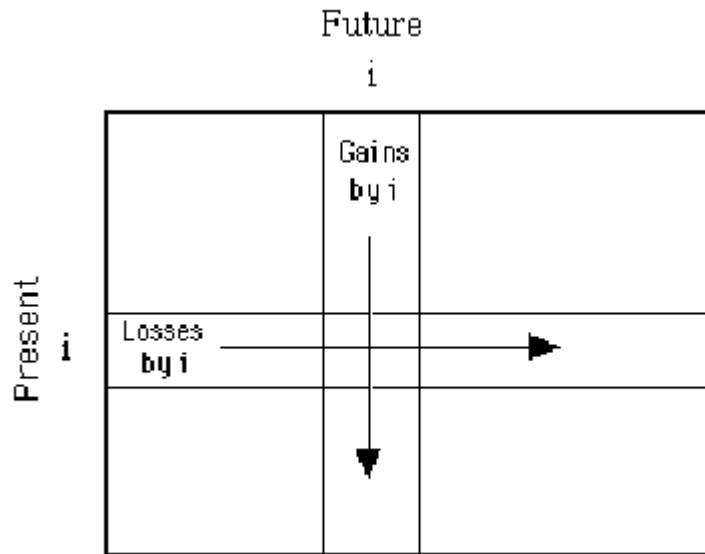


Figure 1. Interpretation of row i (present) and column i (future) in a transition matrix \mathbf{P} . When population i is Type 1, it gains ground. The entries in column i indicate this gain on a population-to-population basis. When population i is Type 2, it suffers losses indicated in the i th row of \mathbf{P} . All rows have unit sum. The column sums may be different.

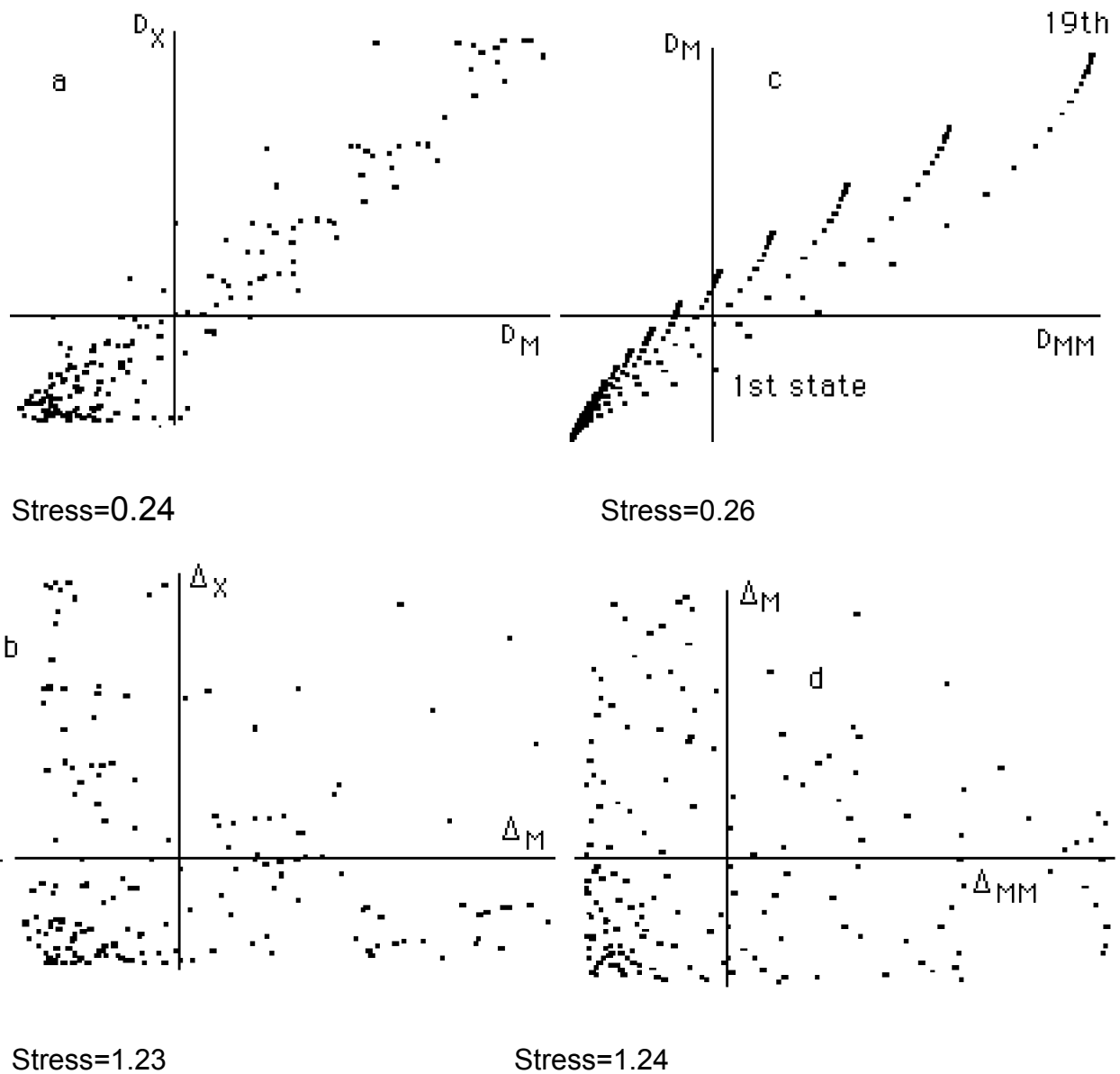


Figure 2. Joint scatter of relevé distances based on analysis of the data in Table 1 (graphs *a* and *b*) and reanalysis of the Markov relevés (graphs *c* and *d*). The horizontal axis depicts the D_M configuration in *a* and *b* and the D_{MM} configuration in *c* and *d*. The vertical axis depicts the D_X configuration in *a* and *b* and the D_M configuration in *c* and *d*. Each graph contains 171 points. Graph *b* and *d* show the effects of randomization. Graph *c* is the signature of the pure Markov process. Graph *a* is the signature of the observed configuration. The latter is similar to the Markov signature with about 12% random variation superimposed. The definition of stress correspond to Eq. 4 in the text.